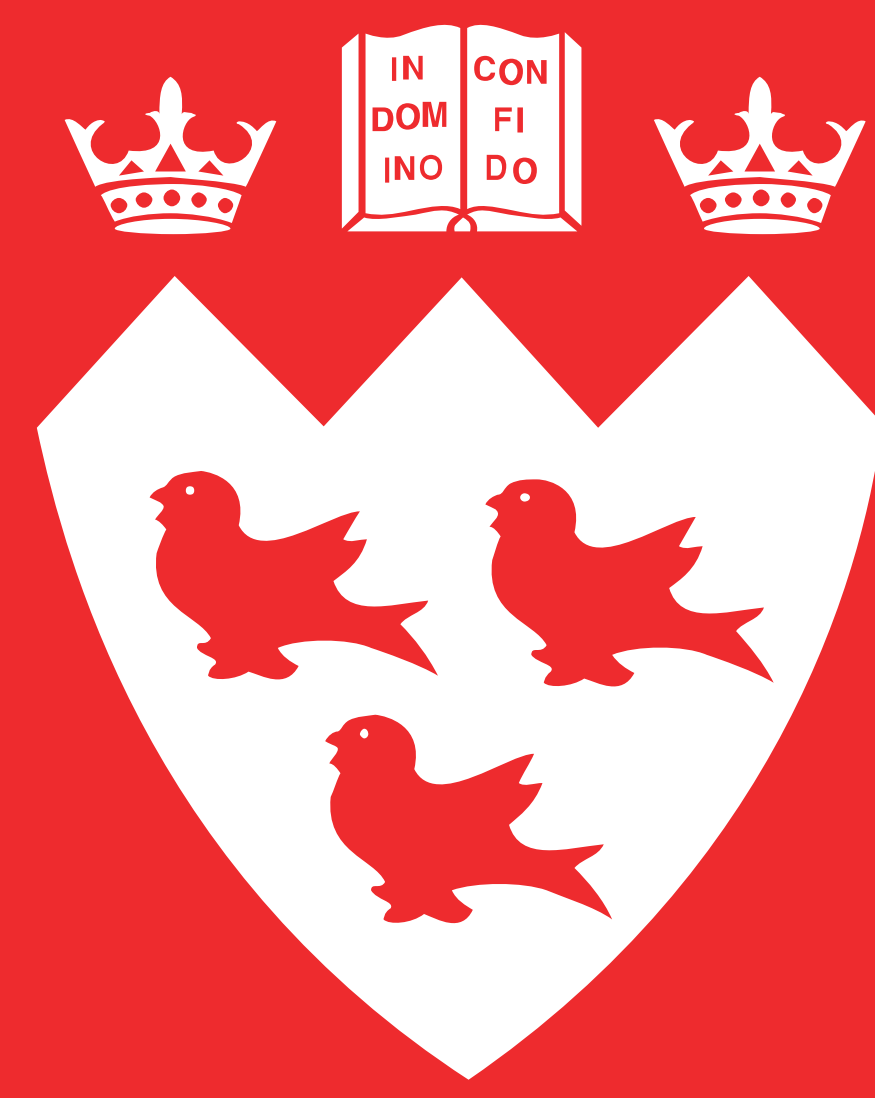# Time- and momentum-resolved phonon population dynamics with ultrafast electron diffuse scattering

L. P. René de Cotret[1], J.-H. Pöhls[1], M. J. Stern[1], M. R. Otto[1], M. Sutton[1], and B. J. Siwick[1,2]

[1] Center for the Physics of Materials, Department of Physics, McGill University
[2] Department of Chemistry, McGill University

Ultrafast electron diffuse scattering

Our inability to fully characterize the nature of elementary excitations and to quantify the strength of their momentum-dependent interactions has been one of the primary barriers to our understanding of these phenomena, particularly in complex anisotropic materials. Ultrafast pump-probe techniques provide an opportunity to study couplings between elementary excitations directly. Photoexcitation can prepare a nonequilibrium distribution of quasiparticles whose subsequent relaxation dynamics and coupling to other degrees of freedom can be followed in the time domain.

In this work we provide a description of the signals contained in ultrafast electron diffuse scattering (UEDS) measurements and a comprehensive and broadly applicable computational method for UEDS data reduction based on density functional perturbation theory (DFPT). Specifically, we present a procedure to recover phonon population dynamics as a function of the phonon branch and wave vector, and a determination of wavevector-dependent (or mode-projected) electron-phonon coupling constants from those phonon population measurements.
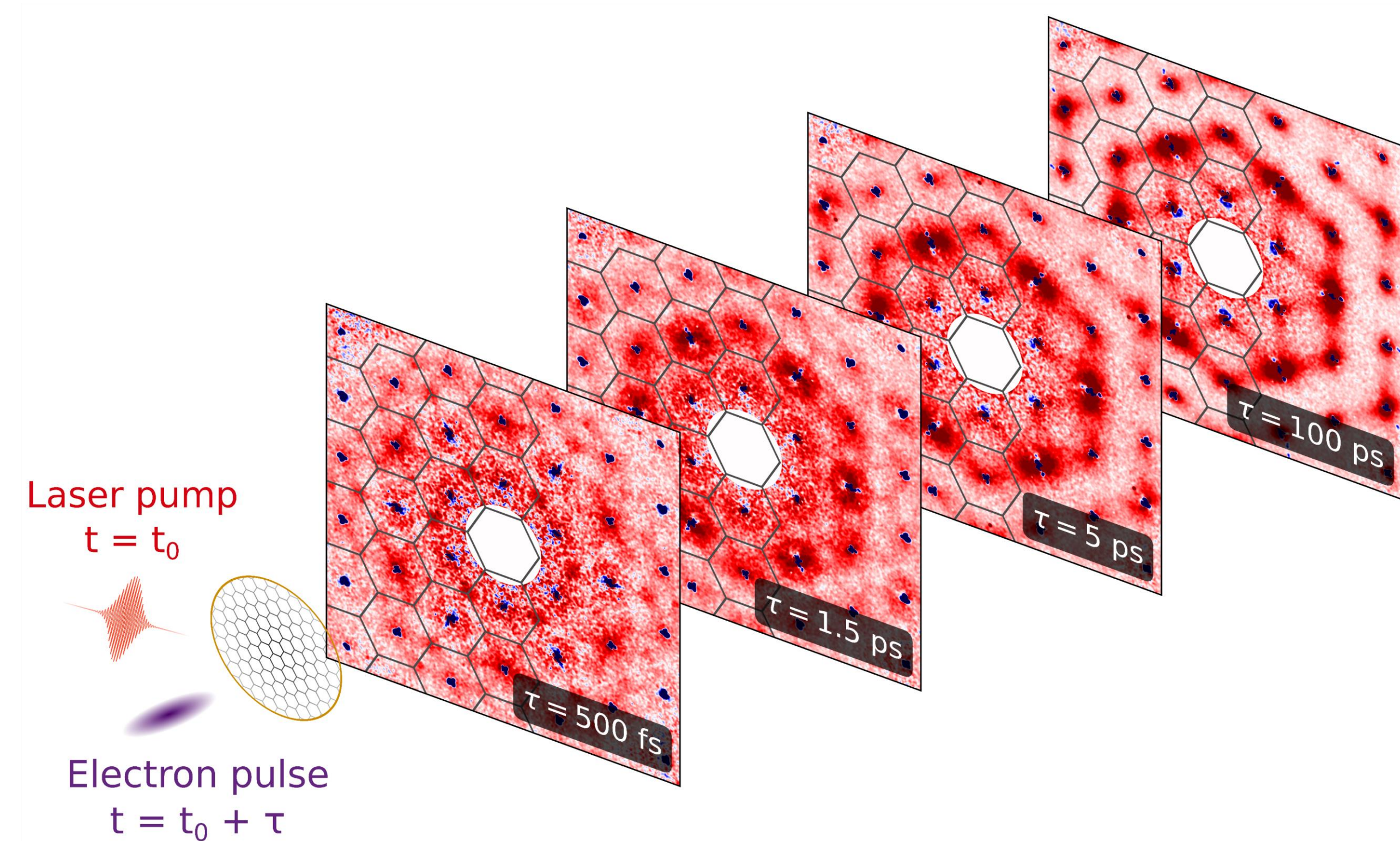

FIGURE 1 Experimental change in transient electron scattering intensity $\Delta I(\mathbf{q}, \tau) = I(\mathbf{q}, t_0 + \tau) - I(\mathbf{q}, t_0)$ of photoexcited graphite for a few representative time-delays, across a wide range of reciprocal space ($|\mathbf{q}| = 12$ Å^{-1}). Negative changes (blue) are limited to Bragg peaks. Positive changes (red) shows diffuse intensity dynamics.

Theory

Similar to x-ray scattering, under the kinematical approximation the measurement of the total scattering intensity $I(\mathbf{q}, t)$ of an electron bunch interacting with a thin film of crystalline material, can be separated into Bragg (elastic) scattering $I_0(\mathbf{q}, t)$ diffuse (nearly-elastic) scattering $I_1(\mathbf{q}, t)$, where the intensity $I_n(\mathbf{q}, t)$ represents the scattered intensity of an electron that interacted with n phonons.

$$I(\mathbf{q}, t) = I_0(\mathbf{q}, t) + I_1(\mathbf{q}, t) + \cdots$$

$$I_1(\mathbf{q}, t) = N_c l_e \sum_j \frac{n_{j,\mathbf{k}}(t) + 1/2}{\omega_{j,\mathbf{k}}(t)} |F_{1j}(\mathbf{q}, t)|^2$$

$$|F_{1j}(\mathbf{q}, t)|^2 = \left| \sum_s e^{-W_s(\mathbf{q}, t)} \frac{f_s(\mathbf{q})}{\sqrt{\mu_s}} (\mathbf{q} \cdot \mathbf{e}_{j,s,\mathbf{k}}) \right|^2$$

$\mathbf{q}$	scattering vector
$\mathbf{H}$	nearest Bragg reflection
$\mathbf{k} = \mathbf{q} - \mathbf{H}$	reduced wavevector
s	atomic index within unit cell
μ_s	atomic mass
$W_s(\mathbf{q}, t)$	Debye-Waller factor
$f_s(\mathbf{q})$	atomic form factor
j	phonon branch index
$\omega_{j,\mathbf{k}}(t)$	phonon frequency
$\mathbf{e}_{j,s,\mathbf{k}}$	phonon polarization
$n_{j,\mathbf{k}}(t)$	phonon population
N_c	Number of scattering events
l_e	Intensity of scattering event

The diffuse scattering intensity contribution of each mode j is weighted by the *one-phonon structure factor* $|F_{1j}(\mathbf{q}, t)|^2$, encoding the locations where the phonon-mode polarization vectors $\{\mathbf{e}_{j,s,\mathbf{k}}\}$ are aligned in such a way that they will contribute to diffuse scattering intensity on the detector, and the strength of the contribution of a single scattering event. The diffuse intensity at $\mathbf{q}$ depends only on the properties of phonons at wavevectors $\mathbf{k} = \mathbf{q} - \mathbf{H}$.

By calculating the one-phonon structure factors, a connection can be made between diffuse intensity $I_1(\mathbf{q}, t)$ and phonon populations $n_{j,\mathbf{k}}(t)$.

One-phonon structure factors

Calculation of one-phonon structure factors requires knowledge of phonon polarization vectors $\{\mathbf{e}_{j,s,\mathbf{k}}\}$ and associated frequencies $\{\omega_{j,\mathbf{k}}\}$. These quantities are computable via density-functional perturbation theory calculation.

Structure relaxation was performed using the plane-wave self-consistent field program PWSCF from the QUANTUM ESPRESSO software suite. The graphite structure was fully relaxed using a $18 \times 18 \times 10$ $\mathbf{k}$-point mesh centered at Γ and force (energy) threshold of 1×10^8 Ry/bohrs (1×10^{-14} Ry). The dynamical matrices were computed on $5 \times 5 \times 3$ $\mathbf{q}$-point grid using a self-consistency threshold of 1×10^8 Ry.

The phonon frequencies and polarization vectors were computed using the PHONON program in the QUANTUM ESPRESSO software suite, using the B86b exchange-coupled Perdew-Burke-Ernzerhof (B86bPBE) generalized gradient approximation (GGA) and the projector augmented-wave (PAW) method. All details are presented in [1].
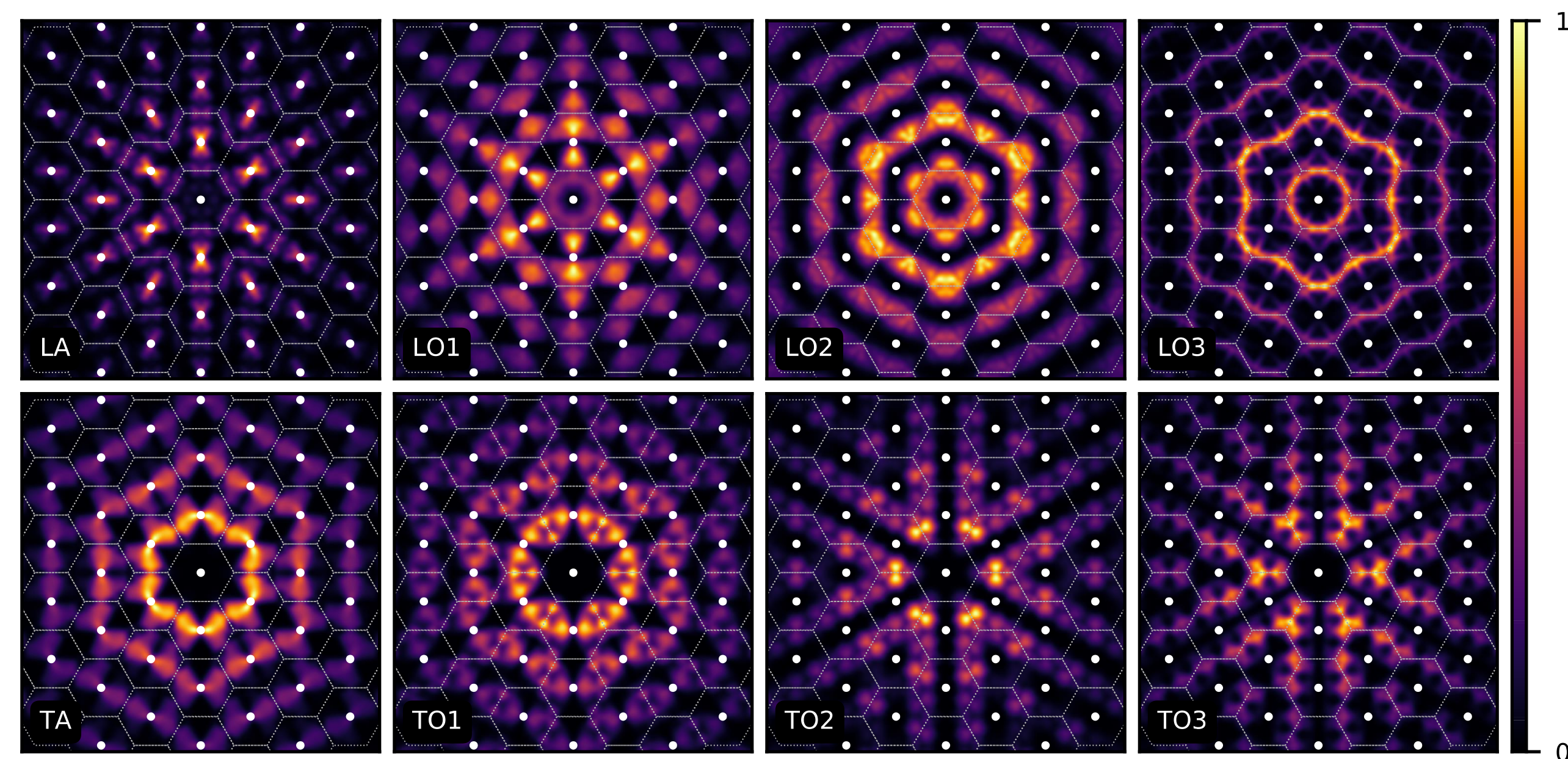

FIGURE 2 Calculated one-phonon structure factors $|F_{1j}(\mathbf{q}, t)|^2$ of all in-plane modes of graphite, at 300 K ($t = t_0$), for $\mathbf{q}$ vectors equivalent to the detector area shown in FIGURE 1. Bright spots indicate locations in reciprocal space where the associated mode j contributes strongly to the diffuse scattering intensity $I_1(\mathbf{q}, t)$. Brillouin zone outlines are overlaid, and their centers (Bragg peaks) are marked with a white dot.

An alternative view of one-phonon structure factors is presented via weighted dispersion curves, an example of which is shown below (FIGURE 4). This presentation allows easy comparison of the relative weights of the one-phonon structure factors along high-symmetry lines for different phonon branches.
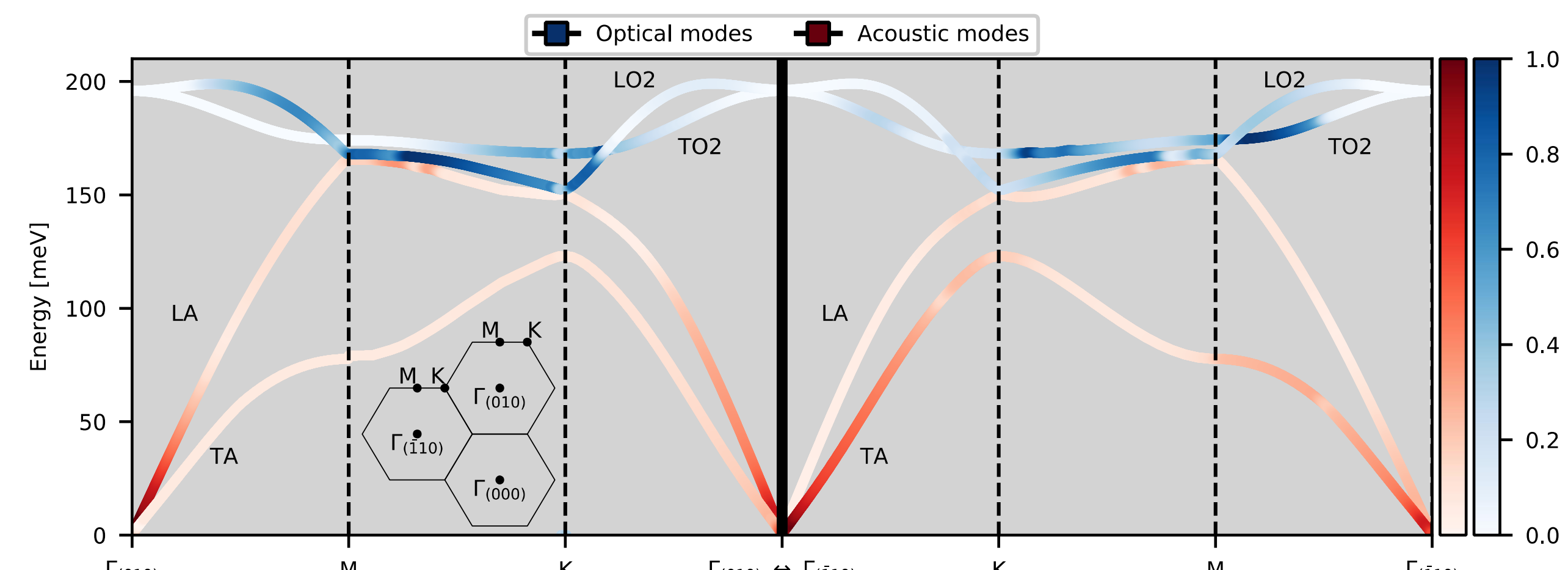

FIGURE 4 Calculated one-phonon structure factors $|F_{1j}(\mathbf{q}, t)|^2$ visualized as weighted dispersion curves for selected in-plane modes of graphite. The color saturation of dispersion curves is proportional to the one-phonon structure factor of the associated mode, at 300 K ($t = t_0$). The left and right paths are shown in a diagram on the bottom left. This figure highlights that one-phonon structure factors values are highly variable, and that their values can differ significantly even when comparing neighbouring Brillouin zones. A striking example of this is the relative strengths of the one-phonon structure factors of LA and TA modes near $\Gamma_{(010)}$ and $\Gamma_{(110)}$. At these locations, the ratio of one-phonon structure factors completely flips, even though the paths are equivalent in the reduced zone scheme.

A cursory inspection of the weighted dispersion curves in FIGURE 4 suggests that there are regions in the Brillouin zone where diffuse intensity is strongly biased toward a single mode (strong scattering selection rule) based on the relative intensities of one-phonon structure factors. Careful analysis reveals that there are very few wavevectors for which a particular phonon mode's one-phonon structure factor is strongly dominant. FIGURE 5 shows that quantitative answers regarding phonon dynamics from UEDS measurements cannot generally be obtained by inspection; at almost any wavevector, at least two phonon modes contribute significantly (>25%) to the transient diffuse scattering intensity.
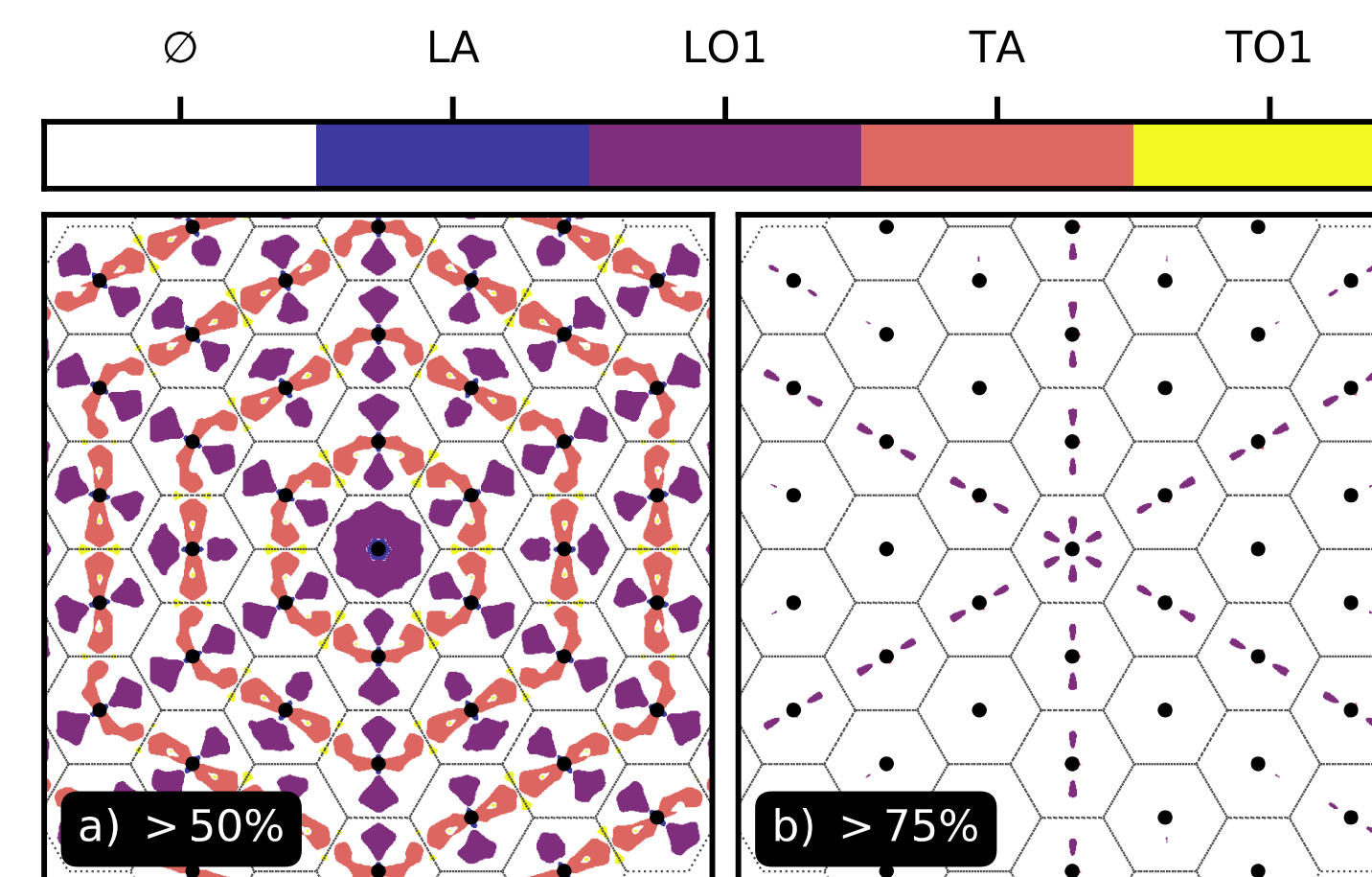

FIGURE 5 Reciprocal-space locations where diffuse intensity is dominated by one mode. **a)** Diffuse intensity is dominated (>50%) by one mode j. White (Ø) regions occur where no phonon mode is dominant. **b)** Locations where diffuse intensity is dominated (>75%) by one mode. This figure shows that there are very few wavevectors where a single mode contributes to diffuse scattering intensity.

Phonon population dynamics

A more robust procedure, must be employed to extract wave-vector- and mode-dependent phonon populations from UEDS intensities. The transient wave-vector-dependent phonon population dynamics $\{\Delta n_{j,\mathbf{k}}(t)\}$ by combining the measurements of $I_1(\mathbf{q}, t)$ with the calculations of one-phonon structure factors and associated quantities presented above.

In graphite, the one-phonon structure factors and phonon frequencies are essentially constant for $\mathbf{k}$ away from Γ, where there is no elastic scattering contribution [1]. Then:

$$\frac{\Delta I(\mathbf{q}, t)}{N_c l_e} = \sum_j \frac{\Delta n_{j,\mathbf{k}}(t)}{\omega_{j,\mathbf{k}}(t_0)} |F_{1j}(\mathbf{q}, t_0)|^2$$

for $\mathbf{k}$ away from Γ. Considering phonon modes $j \in \{1 \dots N\}$, M Brillouin zones are required to make the following system of equations solvable ($M \geq N$):

$$\frac{1}{N_c l_e} \begin{bmatrix} \Delta I(\mathbf{k} + \mathbf{H}_1, t) \\ \vdots \\ \Delta I(\mathbf{k} + \mathbf{H}_M, t) \end{bmatrix} = \begin{bmatrix} |F_{11}(\mathbf{k} + \mathbf{H}_1, t_0)|^2 & \cdots & |F_{1N}(\mathbf{k} + \mathbf{H}_1, t_0)|^2 \\ \vdots & & \vdots \\ |F_{11}(\mathbf{k} + \mathbf{H}_M, t_0)|^2 & \cdots & |F_{1N}(\mathbf{k} + \mathbf{H}_M, t_0)|^2 \end{bmatrix} \begin{bmatrix} \Delta n_{1,\mathbf{k}}(t)/\omega_{1,\mathbf{k}}(t_0) \\ \vdots \\ \Delta n_{N,\mathbf{k}}(t)/\omega_{N,\mathbf{k}}(t_0) \end{bmatrix}$$

The system of equations above must be repeated for every reduced scattering vector $\mathbf{k}$. The solution for the system of equations above, across most of the Brillouin zone, is presented in FIGURE 6 for a few relevant phonon modes.
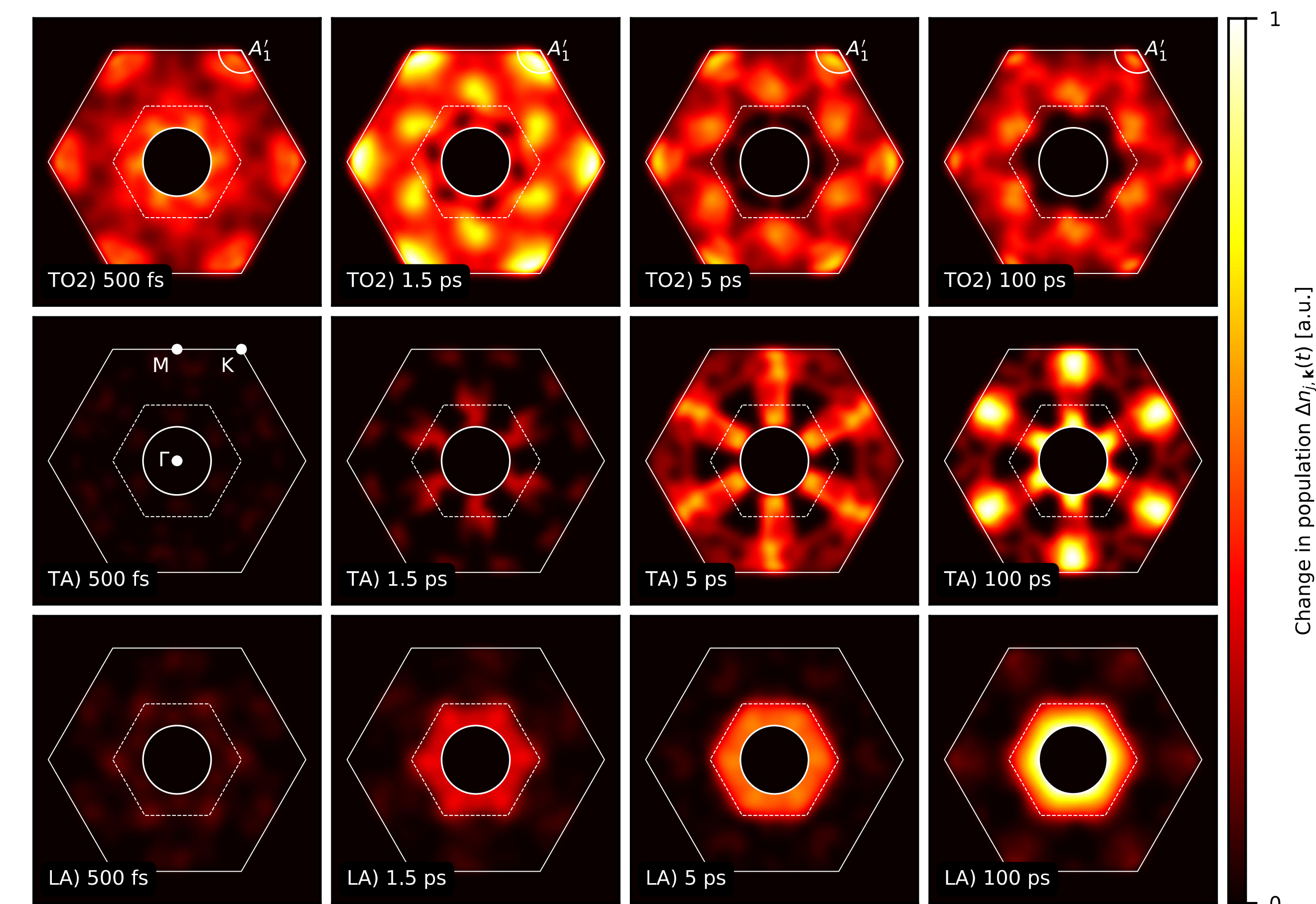

FIGURE 6 Experimental change in transient population, across the Brillouin zone, of relevant in-plane modes of graphite following photoexcitation. The decomposition of transient diffuse intensity (FIGURE 1) yields stable solutions for $|\mathbf{k}| > 0.45$ Å^{-1}. The Brillouin zone midpoints are shown with a dashed hexagon. The differential A_1' phonon population is highlighted by a circular arc centered at $\mathbf{K}$ in the TO2 phonon population images; its dynamics are discussed below.

Mode-projected couplings

Phonon population transients are related to mode-specific effective temperatures $T_{ph,j}$ after initial electron thermalization ($t > 100$ fs):

$$n_{j,\mathbf{k}}(t) \propto \left[\exp\left(\frac{\hbar \omega_{j,\mathbf{k}}}{k_B T_{ph,j}(t)} \right) - 1 \right]^{-1} = \frac{k_B T_{ph,j}(t)}{\hbar \omega_{j,\mathbf{k}}} - \frac{1}{2} + o(T_{ph,j}^{-1}(t))$$

This relation can be used to describe the exchange of energy between electrons and specific phonons modes by making use of a generalized two-temperature model, the nonthermal lattice model [3]. The case of coupling to/from the A_1' mode is described as follows:

$$C_e(T_e)\dot{T}_e = f(t - t_0) - G_{e,A_1'}(T_e - T_{A_1'}) - G_{e,l}(T_e - T_l)$$

$$C_{A_1'}(T_{A_1'})\dot{T}_{A_1'} = G_{e,A_1'}(T_e - T_{A_1'}) - G_{A_1',l}(T_{A_1'} - T_l)$$

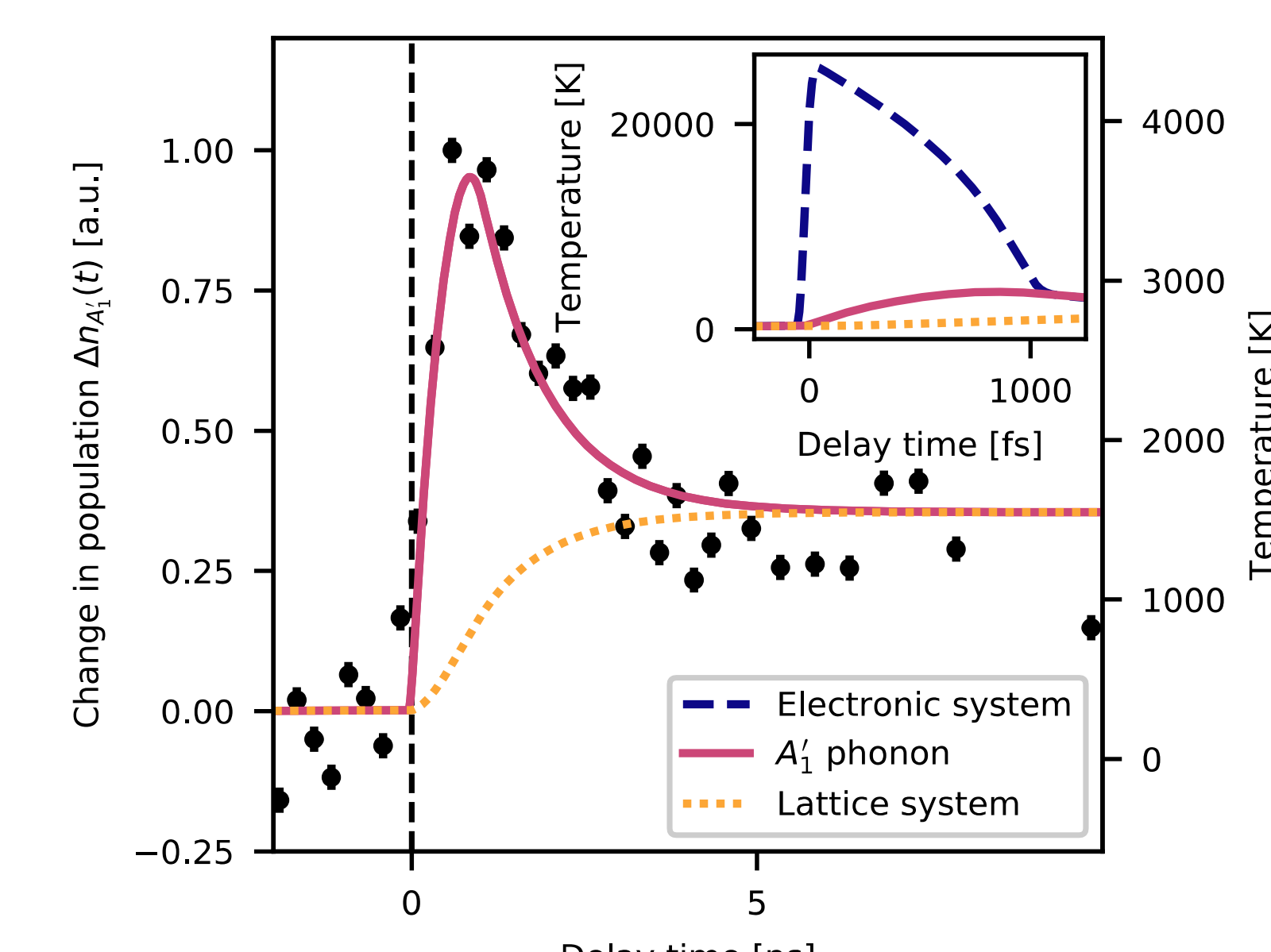$$C_l(T_l)\dot{T}_l = G_{e,l}(T_e - T_l) + G_{A_1',l}(T_{A_1'} - T_l)$$

T_e	Electronic temperature
$T_{A_1'}$	A_1' mode temperature
T_l	Other modes temperature
$\{C_x\}$	Heat capacities
$\{G_{x,y}\}$	Coupling strengths

FIGURE 7 Evolution of the A_1' mode population in graphite after ultrafast photoexcitation. Differential population measurement of A_1', shown in black (circle), is obtained from the integration of the TO2 mode population in a circular arc centered at $\mathbf{K}$, visible in FIGURE 6. The fit to the population change is shown in pink (solid). The effective temperature of the modes in which the A_1' phonon can decay is shown as an orange (dotted) line. **Inset:** temperature dynamics at early times show that thermalization between the electronic system (purple, dashed) and the A_1' phonon population (pink, solid) is very fast, indicative of strong electron-phonon coupling.

Coupling strength W m^{-3} K^{-1}	$G_{e,A_1'}$	$G_{A_1',l}$	$G_{e,l}$
	$(6.8 \pm 0.3) \times 10^{17}$	$(8.0 \pm 0.5) \times 10^{17}$	$(0.0 \pm 6.0) \times 10^{15}$

The fit to a nonthermal lattice model results in the coupling strengths above. In particular, the coupling strength $G_{e,A_1'}$ between electrons and the A_1' mode corresponds to a mode-projected electron-phonon coupling value of (0.035 ± 0.001) eV^2. These results are in excellent agreement with recent tr-ARPES measurements and simulations [4].

Conclusion

UEDS provides direct access to wave-vector-resolved, nonequilibrium phonon populations and is, in this sense, a lattice-dynamical analog of time-resolved angle-resolved photoelectron spectroscopy (tr-ARPES). A robust and generally applicable UEDS data reduction method has been described that provides detailed information on transient changes in phonon populations across the entire Brillouin zone that follow photoexcitation in single-crystalline materials.

References

[1] L. P. René de Cotret, J.-H. Pöhls, M. J. Stern, M. R. Otto, M. Sutton, and B. J. Siwick, *Time- and momentum-resolved phonon population dynamics with ultrafast electron diffuse scattering*, Phys. Rev. B **100** (2019)

[2] M. J. Stern, L. P. René de Cotret, M. R. Otto, R. P. Chatelain, J.-P. Boisvert, M. Sutton, and B. J. Siwick, *Mapping momentum-dependent electron-phonon coupling and non-equilibrium phonon dynamics with ultrafast electron diffuse scattering*, Phys. Rev. B **97** (2018)

[3] L. Waldecker, R. Bertoni, R. Ernstorfer, and J. Vorberger, *Electron-phonon coupling and energy flow in a simple metal beyond the two-temperature approximation*, Phys. Rev. X **6**, 021003 (2016).

[4] M.X. Na, A. K. Mills, F. Boschini, *et al*, *Direct determination of mode-projected electron-phonon coupling in the time domain*, Science **366** (2019)